DEVELOPMENT OF OPTIMUM DESIGN CONFIGURATION AND PERFORMANCE FOR VERTICAL AXIS WIND TURBINE

FEASIBILITY ANALYSIS AND FINAL EISG REPORT

Prepared For:
California Energy Commission
Energy Innovations Small Grant Program

Prepared By:
Hamid R. Rahai
California State University, Long Beach

May 2005
CEC-500-2005-084

ENERGY INNOVATIONS SMALL GRANT (EISG) PROGRAM

FEASIBILITY ANALYSIS REPORT (FAR)

DEVELOPMENT OF OPTIMUM DESIGN CONFIGURATION AND PERFORMANCE FOR VERTICAL AXIS WIND TURBINE

EISG AWARDEE
Mechanical and Aerospace Engineering Department
California State University, Long Beach
1250 Bellflower Blvd
Long Beach, Ca. 90840
Phone: (562) 985-4407
Email: rahai@csulb.edu
Principal Investigator: Hamid R. Rahai

Grant #: 00-17
Grant Funding: $69,781
Term: February 2001 – November 2002
PIER Subject Area: Renewable Energy Technologies

Printed on Wednesday, April 27, 2005 at 2:32 PM

LEGAL NOTICE

PREFACE

The Public Interest Energy Research (PIER) Program supports public interest energy research and development that will help improve the quality of life in California by bringing environmentally safe, affordable and reliable energy services and products to the marketplace.

The PIER Program, managed by the California Energy Commission (Commission), annually awards up to $62 million of which $2 million/year is allocated to the Energy Innovation Small Grant (EISG) Program for grants. The EISG Program is administered by the San Diego State University Foundation under contract to the California State University, which is under contract to the Commission.

The EISG Program conducts four solicitations a year and awards grants up to $75,000 for promising proof-of-concept energy research.

PIER funding efforts are focused on the following six RD&D program areas:

- Residential and Commercial Building End-Use Energy Efficiency
- Industrial/Agricultural/Water End-Use Energy Efficiency
- Renewable Energy Technologies
- Environmentally-Preferred Advanced Generation
- Energy-Related Environmental Research
- Strategic Energy Research

The EISG Program Administrator is required by contract to generate and deliver to the Commission a Feasibility Analysis Report (FAR) on all completed grant projects. The purpose of the FAR is to provide a concise summary and independent assessment of the grant project using the Stages and Gates methodology in order to provide the Commission and the general public with information that would assist in making follow-on funding decisions (as presented in the Independent Assessment section).

The FAR is organized into the following sections:

- Executive Summary
- Stages and Gates Methodology
- Independent Assessment
- Appendices
    - Appendix A: Final Report (under separate cover)
    - Appendix B: Awardee Rebuttal to Independent Assessment (Awardee option)

For more information on the EISG Program or to download a copy of the FAR, please visit the EISG program page on the Commission's Web site at:
http://www.energy.ca.gov/research/innovations

or contact the EISG Program Administrator at (619) 594-1049 or email eisgp@energy.state.ca.us.

For more information on the overall PIER Program, please visit the Commission's Web site at http://www.energy.ca.gov/research/index.html.

Development Of Optimum Design Configuration And Performance For Vertical Axis Wind Turbine

EISG # 00-17

Awardee:	California State University, Long Beach
Principal Investigator:	Hamid R. Rahai
PI Contact Info:	(562) 985-4407; rahai@sculb.edu
Grant Funding:	$69, 781
Grant Term:	February 2001-November 2002

Introduction

This project was undertaken to improve the efficiency of vertical axis wind turbines with the expectation that the inherently simple vertical axis turbines could be manufactured at low cost, leading to their widespread use. The research proposal noted that small units could be manufactured for distributed generation of electricity in residential and commercial locations. The units would be grid connected to take advantage of net metering and would provide pollution free generation of electricity using a renewable resource at a cost competitive with power supplied by the grid.

The researcher estimates that a moderate sized residential unit would generate 2700 kWh per year and that the low cost of the unit would allow a simple payback of investment from energy savings in three years. If 100,000 of these small wind turbines were installed in California they would eliminate the annual generation and release of nearly 10 tons of oxides of nitrogen and over 13 tons of carbon monoxide gas. These calculations are based on California's 2007 air emission standards for natural gas burning distributed generation. Displacing older generators would result in greater environmental benefits.

The simplest vertical axis wind turbine is called the Savonius wind turbine. Operation of the Savonius wind turbine is based on the difference of the drag of its semi-spherical vanes, depending on whether the wind is striking the convex or the concave part of the vane. The advantage of this type of wind turbine is that it is self-starting and relatively independent of the wind direction. It is simple to design and has relatively low construction cost. However it has low efficiency.

The approach taken by this project was to improve the efficiency of the vertical axis (Savonius-type) wind turbine by modifying the blades. The blade shape was iteratively designed using Computational Fluid Dynamics software embedded within a torque maximization program using the Trans Finite Interpolation method, (see appendix A). A scale model vertical axis wind turbine featuring the optimized blade design was constructed and tested in the Boeing/CSULB low speed wind tunnel. Wind tunnel tests confirmed a 40% increase in peak power coefficients over prior art.

Objectives

The goal of this project was to determine the feasibility of developing a high efficiency Savonius-type vertical axis wind turbine by modifying the blade (airfoil) shape. The researcher established the following project objectives:

1. Increase the efficiency of the vertical axis wind turbine design 20% to 30% by applying computational fluid dynamics (CFD) software to optimize the airfoil shape
2. Experimentally verify the design by testing scale model wind turbines in the Boeing/CSULB low speed wind tunnel

Outcomes

1. The researcher used CFD software and an optimizer routine for the shape-optimization process. Results of this study showed nearly 27% improvement in the torque coefficient for both single and two-blade configurations with the optimized geometry. The computations also led the researcher to investigate the placement of slots in the airfoils at the location where maximum flow separation was observed at high angles of attack. The improvement in the torque coefficient without the slots was greater than that with the slots.
2. The researcher fabricated two small-scale vertical axis wind turbines, one with and one without span-wise slots. They were tested in the Boeing/CSULB low speed wind tunnel at three free-stream mean velocities: 6.8, 8.0, and 9.75 m/sec (15.2, 17.9, and 21.8 miles/hr). The experiments were performed for both zero and 48% overlap of the blades. Torque was measured directly using an electric dynamometer. Results showed nearly 40 % and17% improvement in power coefficient for the optimized blades without and with the slots respectively. The conditions for these results were zero overlap at the mean velocity of 6.8 m/sec.
3. It was determined the optimized wind turbine operated more efficiently than the Savonius wind turbine at all tip speed ratios[1]. A significant result of this study was the determination that the optimized wind turbine operated efficiently at a much higher rotation rate than the Savonius wind turbine could operate. The Savonius wind turbine provides its maximum power coefficient (about 30%) at a tip speed ratio of approximately 1.0. The optimized wind turbine with no slots and zero overlap produced a power coefficient greater than 40%[2] at a tip speed ratio of 1.6. At this tip speed ratio the Savonius turbine power coefficient dropped to below 5%.

Conclusions

1. This project confirmed the feasibility of using computational fluid dynamics software to aid the design of single blade, vertical axis, wind turbine airfoils. It is reasonable to expect investigations of multi-bladed vertical axis wind turbines could be accomplished using the same computational approach. CFD software is already used in other energy products including centrifugal pumps vanes and gas turbine compressor and turbine blades.
2. Wind tunnel testing confirmed the most efficient vertical axis wind turbine design used the optimized airfoils without slots and mounted with no overlap. This design demonstrates high efficiency over the range of wind speeds from 6.8 m/s to 9.75 m/s.

[1] Tip Speed Ratio – The speed of the outer edge or tip of the rotor divided by the speed of the wind.
[2] Power Coefficient - The portion of the power of the wind that the machine is able to capture.

3. The optimized wind turbine provided higher power coefficients over a broad operating range. The characteristic of providing power at much higher tip speed ratios potentially increases the total power produced by the turbine. The optimized wind turbine provided optimum power at a tip speed ratio of 1.6. This is 60% faster than the Savonius wind turbine. For this reason the redesigned turbine provides 60% more power than a Savonius turbine operating at a tip speed ratio of 1.0. Coupled with the approximate 33% increase in the power coefficient, the new design could produce over twice the power of the conventional Savonius wind turbine under comparable conditions.

Benefits to California

Because the researcher saw a market in small vertical-axis wind turbines he did not make absolute comparisons between the optimized vertical axis wind turbine and the conventional horizontal axis wind turbines that are commercially available. The researcher speculated that a one-kilowatt vertical-axis wind turbine generator system could be built for $300. To ascertain the value of this research to the California ratepayer, the PA requires a more accurate estimate of the cost to construct and maintain a vertical axis wind turbine with optimized blades. This estimate could assume deployment in one of California's traditional wind regions or in high-density urban areas. The improved design vertical axis wind turbine could prove to be more cost effective than horizontal axis turbines because of the improvements in blade design and the elimination of equipment required to maintain a horizontal axis machine heading into the wind. Any improvements to the cost and durability of wind turbine generation systems could have significant favorable impacts on the California ratepayer. These benefits include: lower cost renewable resource electricity; increased production of renewable resource electricity, reduced air pollution; and increased energy security through local electricity production.

Recommendations

This project demonstrated the utility of using CFD to redesign the blades of vertical axis wind turbines. The redesigned wind turbine can generate electric power at relatively moderate wind speed with an efficiency that is near that of a comparable horizontal axis wind turbine. The PA recommends that a thorough cost analysis be completed for the redesigned vertical axis turbine. That study should focus on production costs to build and install it in selected markets. A person familiar with maintaining wind turbines in a California wind region should then evaluate maintenance costs for the vertical axis machine. If these studies indicate a significant life cycle cost advantage, the researcher should team with a wind generation company to field-test a CFD-improved vertical axis wind turbine at a power level of 1 KW or more at wind speeds of 10-15 miles/hr. The PA recommends significant instrumentation be applied to that demonstration turbine to ascertain it performance, sensitivity to environmental contamination, and noise levels.

Stages and Gates Methodology

The California Energy Commission utilizes a stages and gates methodology for assessing a project's level of development and for making project management decisions. For research and development projects to be successful they need to address several key activities in a coordinated fashion as they progress through the various stages of development. The activities of the stages and gates process are typically tailored to fit a specific industry and in the case of PIER the activities were tailored to be appropriate for a publicly funded energy research and development program. In total there are seven types of activities that are tracked across eight stages of development as represented in the matrix below.

Development Stage/Activity Matrix

	Stage 1	Stage 2	Stage 3	Stage 4	Stage 5	Stage 6	Stage 7	Stage 8
Activity 1								
Activity 2								
Activity 3								
Activity 4								
Activity 5								
Activity 6								
Activity 7								

A description the PIER Stages and Gates approach may be found under "Active Award Document Resources" at: http://www.energy.ca.gov/research/innovations and are summarized here.

As the matrix implies, as a project progresses through the stages of development, the work activities associated with each stage needs to be advanced in a coordinated fashion. The EISG program primarily targets projects that seek to complete Stage 3 activities with the highest priority given to establishing technical feasibility. Shaded cells in the matrix above require no activity, assuming prior stage activity has been completed. The development stages and development activities are identified below.

Development Stages:	Development Activities:
Stage 1: Idea Generation & Work Statement Development	Activity 1: Marketing / Connection to Market
Stage 2: Technical and Market Analysis	Activity 2: Engineering / Technical
Stage 3: Research & Bench Scale Testing	Activity 3: Legal / Contractual
Stage 4: Technology Development and Field Experiments	Activity 4: Environmental, Safety, and Other Risk Assessments / Quality Plans
Stage 5: Product Development and Field Testing	Activity 5: Strategic Planning / PIER Fit - Critical Path Analysis
Stage 6: Demonstration and Full-Scale Testing	Activity 6: Production Readiness / Commercialization
Stage 7: Market Transformation	Activity 7: Public Benefits / Cost
Stage 8: Commercialization	

Independent Assessment

For the research under evaluation, the Program Administrator assessed the level of development for each activity tracked by the Stages and Gates methodology. This assessment is summarized in the Development Assessment Matrix below. Shaded bars are used to represent the assessed level of development for each activity as related to the development stages. Our assessment is based entirely on the information provided in the course of this project, and the final report. Hence it is only accurate to the extent that all current and past work related to the development activities are reported.

Development Assessment Matrix

Stages / Activity	1 Idea Generation	2 Technical & Market Analysis	3 Research	4 Technology Develop-ment	5 Product Develop-ment	6 Demon-stration	7 Market Transfor-mation	8 Commer-cialization
Marketing								
Engineering / Technical								
Legal/ Contractual								
Risk Assess/ Quality Plans								
Strategic								
Production. Readiness/								
Public Benefits/ Cost								

The Program Administrator's assessment was based on the following supporting details:

Marketing/Connection to the Market

The researcher reviewed available market opportunities. He suggested placement of vertical axis wind turbines on or near residential and commercial buildings, along beaches, and also in the right-of-way of major freeways. The PA commends the researcher for seeking increased local generation of renewable energy. Additional work must be done to show that significant wind resource exists at these sites and that they can be permitted for construction. The researcher should also indicate how the development of local wind turbine generators could be financed.

Engineering/Technical

The researcher completed a CFD optimization of blades for a vertical axis wind turbine. The results indicate significant increase in efficiency over conventional vertical axis turbines. Cost to produce and maintain the improved units could be favorable, but they need to be accurately assessed. If the potential life-cycle energy costs appear to be favorable, the research should proceed to a field test of a 1 kW system. Field-testing should be designed to evaluate reliability and sensitivity to environmental contaminants. No plan for field-testing was submitted in the final report.

Legal/Contractual

The researcher has filed a disclosure for a patent on the design of the new wind turbine.

Environmental, Safety, Risk Assessments/ Quality Plans

Quality Plans include Reliability Analysis, Failure Mode Analysis, Manufacturability, Cost and Maintainability Analyses, Hazard Analysis, Coordinated Test Plan, and Product Safety and Environmental The researcher has assessed some of the technical risk factors. However significant work remains on the other required plans. Work on these plans should begin in the next phase of work.

Strategic

This product has no known critical dependencies on other projects under development by PIER or elsewhere.

Production Readiness/Commercialization

There is no indication the researcher has a production readiness plan, a commercialization partner, or a business plan. Potential product cost is highly dependent on materials, manufacturing processes, and production volumes. A production partner could provide significant aid in developing the needed business plan.

Public Benefits

Public benefits derived from PIER research and development are assessed within the following context:

- Reduced environmental impacts of the California electricity supply or transmission or distribution system
- Increased public safety of the California electricity system
- Increased reliability of the California electricity system
- Increased affordability of electricity in California

The primary benefit to the ratepayer from this research is the increased affordability of a renewable energy resource. Implementation of the project innovation could increase renewable energy production and reduce air emissions.

A high-efficiency vertical axis wind turbine can be designed for an output of one-kilowatt power output in mild wind speeds of 10-15 miles/hr. These wind speeds exist in some coastal regions for more than six months of a year. Assuming an average of 15 hours of wind per day during a 6 month period, the total annual energy generated by a single wind turbine could be 2,700 kWh. At an assumed cost of 3.5 cents per KWh, the total value of electricity produced could be about $95. In niche markets the value of the electricity could be significantly higher, producing faster payback times. Teamed with photovoltaic generation and energy storage, the one-kilowatt wind turbine could displace electricity now costing residential and commercial customers about $0.15/kWh. The displacement of grid electricity, especially during peak hours, could relieve grid congestion and thus lower costs to all California ratepayers.

Program Administrator Assessment

After taking into consideration: (a) research findings in the grant project, (b) overall development status as determined by stages and gates, and (c) relevance of the technology to California and the PIER program, the Program Administrator has determined that the proposed technology should be considered for follow-on funding within the PIER program.

Receiving follow-on funding ultimately depends upon: (a) availability of funds, (b) submission of a proposal in response to an invitation or solicitation, and (c) successful evaluation of the proposal.

Appendix A: Final Report (under separate cover)

Appendix B: Awardee Rebuttal to Independent Assessment (none submitted)

Appendix A to FAR 00-17

ENERGY INNOVATIONS SMALL GRANT (EISG) PROGRAM

EISG FINAL REPORT

DEVELOPMENT OF OPTIMUM DESIGN CONFIGURATION AND PERFORMANCE FOR VERTICAL AXIS WIND TURBINE

EISG AWARDEE

Mechanical and Aerospace Engineering Department
CALIFORNIA SATE UNIVERSITY, LONG BEACH
1250 Bellflower Blvd
Long Beach, Ca. 90840.
Phone: (562) 985-4407
Email: rahai@csulb.edu

AUTHORS

Hamid R. Rahai, Principal Investigator
Hamid Hefazi, Co-Principal Investigator

Grant #: 00-17
Grant Funding: $69,781
Term: February 2001 – January 2002
PIER Subject Area: Renewable Energy Technologies

Legal Notice

Inquires related to this final report should be directed to the Awardee (see contact information on cover page) or the EISG Program Administrator at (619) 594-1049 or email eisgp@energy.state.ca.us.

Acknowledgement Page

The authors would like to thank Mike Fritz, Tadashi Murayama, Adline Schmitz, and Huy Hoang of Mechanical and Aerospace Engineering Department for their invaluable contributions.

Table of Contents

List of Figures

Page

Abstract

A general aerodynamic optimization method was used to improve the torque characteristics of a Split-Savonius type vertical axis wind turbine. NASA INS2D software was used to compute the aerodynamic performances required to evaluate the torque characteristics. A decomposition, deformation, and reassembly method was developed to accommodate the variable geometry of the blade during the optimization process. The deformation of the grid was accomplished by a modified version of the Transfinite Interpolation (TFI) method. The method is first applied to a single blade of the turbine and yields a 27% improvement in overall torque. Further analyses were performed on a single blade with a spanwise slot and two-blade configuration with and without the slots and results indicated more than 10% further improvement in the overall torque with the slots in place.

Two small scale prototype double-blades turbines with and without the spanwise slots were built and tested in the Boeing/CSULB low speed wind tunnel at three free stream mean velocities of 6.8, 8, and 9.75 m/sec which correspond to Reynolds numbers based on cord length of 12.25×10^4, 14.4×10^4, 17.6×10^4 respectively. The experiments were performed for blades at zero and 48% overlap conditions. Results show that at the free stream mean velocity of 6.8 m/sec, for the zero overlap condition, the peak power coefficients for the optimized blade with and without the slots are respectively 17% and 40% higher than the corresponding value for the high efficiency Benesh airfoil. The continuous increase in the power coefficients for the optimized blades extend to a tip speed ratio of 1.6, much higher than the range observed for the Benesh airfoil.

Key Words: (vertical axis wind turbine, wind energy, thin airfoil optimization, aerodynamic optimization, wind turbine rotor optimization)

Executive Summary

Wind turbines have been used extensively for power generation. Other than moderate noise pollution, they are pollution free and have relative low operating costs. However, the present wind turbines have high initial investment cost and their performance depends on wind direction into which they have to be continuously positioned for maximum power output.

There are two general types of wind turbines, the horizontal axis, and the vertical axis wind turbines where each has different configuration. The simplest of all is a vertical axis wind turbine, which is called the Savonius wind turbine. The principle of operation of Savonius wind turbine machine is based on the difference of the drag of semi-circular vanes, depending on whether the wind is striking the convex or the concave part of the vane. The advantage of this type of machine is that it is self-starting and thus relatively independent of the wind direction and is simple to design and has low construction cost. However, previous extensive experimental studies have shown that it has low efficiency.

To improve the efficiency of the Savonuis turbine requires modification of the blades. Thin highly cambered airfoils have shown to have higher drag than the thick sections of less cambered ones. For thin airfoils, there are contributions of the lift to the drag force, and the torque for the turbine is the summation of the drag and lift forces and not just the drag alone. Thus any geometrical or design modification that can increase the torques will result in efficiency improvement.

The objective of our investigations was to develop a high efficiency vertical axis wind turbine with blade shape modification. A Computational Fluid Dynamic (CFD) code along with various objective functions and an optimizer routine were used for the shape optimization process. The objective of this part of the study was to obtain a shape configuration that would produce a high torque for the vertical axis wind turbines. For both single and two-blade configurations with the optimized geometry, results of this part of the investigation showed nearly 27% improvement in the torque coefficient.

Previous studies have shown that multi-element airfoils produce higher lift. Since significant part of our increase in torque was from lift, we also analyzed flow characteristics and overall torque of our optimized single and double blade configurations with and without spanwise slots. The slots were placed at the location where maximum flow separation was observed at high angles of attack. This configuration is very similar to the multi-element airfoils but has higher rigidity, which is more suitable for the vertical axis wind turbines. The improvement in the torque coefficient with the slots was not as significant as when the slots were not in place.

The second part of the investigations was focused on experimental verification of the numerical results. Two small-scale vertical axis wind turbine were fabricated with and without the spanwise slots and they were tested in the Boeing/CSULB low speed wind tunnel at three free stream mean velocities of 6.8, 8.0, and 9.75 m/sec (15.2, 17.9, and 21.8 miles/hr). The experiments were performed for both zero and 48% overlap conditions. Torque was measured directly using an electric dynamometer, which was attached to the turbine via a belt-pulley arrangement outside the wind tunnel. Results showed nearly 17% and 40% improvement in power coefficient for the optimized blades with and without the slots respectively; at zero overlap condition, at the mean velocity of 6.8 m/sec.

Our investigation has shown that the vertical axis wind turbines with optimized blade configuration can generate electric power at relatively moderate wind speed with an efficiency that is nearly comparable with the horizontal axis wind turbines. Considering the low initial investment and operating cost, we recommend development and field-testing of two large vertical axis wind turbines with the optimized blade configuration, which can generate 1 KW of power at moderate wind speeds of 10-15 miles/hr. These turbines can be tested near the beach area where continuous moderate wind exists for most of the year. They can also be tested on the top of the tall commercial and residential buildings where higher wind shear will produce nearly continuous power for most of the year.
Various scales of these wind turbines can be constructed for different applications. They can be used to generate electricity for lighting along the beaches in both public and private properties. They can be installed between the freeways where the wind shear from passing cars and trucks will rotate these turbines to generate enough power to light under the overpasses and between the freeways. They can be produced at small scales to generate power for boats and RVs at moderate wind speeds in stationary condition. Overall there are substantial savings and public benefits for California from these high efficiency independent vertical axis wind turbines.

Introduction

Thin highly cambered airfoils have shown to have higher drag than thick sections of less camber. Milgram [1] presents section data for thin highly cambered airfoils with sharp edges in

incompressible flow. His results show that at the ideal angle of attack as given by the airfoil theory, the thin, highly cambered sections have as much as five times more drag than the thick sections of less camber.

Liebeck [2,3] presents results of theoretical and experimental studies for designing a single element airfoil, which provides the maximum possible lift without separation at the design angle of attack in an incompressible flow. His approach was to obtain first a set of optimum velocity distributions using the boundary layer theory and the calculus of variation and then adjusting these distributions to obtain realistic and practical airfoil shapes. His theoretical results include a very thin high lift airfoil, which could increase the lift by more than three fold. However, this airfoil had leading edge separation at the design angle of attack. When the airfoil leading edge was modified, the increase in lift was slightly less, but flow separation was removed. His experimental investigation of two modified airfoils confirmed the theoretical predications of increase in lift without flow separation. Furthermore, the results were independent of the tested Reynolds numbers of 1 to 3 millions.

Modi and Fernando [4] presented results of extensive wind tunnel tests on a vertical axis Savonius wind turbine. Figure 1a shows a typical vertical axis Savonius wind turbine. In their study, the turbine blades were modified to increase efficiency. The blades consisted of two arcs connected to two straight end plates. The parameters investigated were blade overlap, blade gap size, aspect ratio, blade shape parameters and blade arc angle. Their results indicate that the Savonius rotor is not just a pure drag device, but at small angle of attacks, it behaves similar to a slender body with lift contributing to power. They presented optimum values for the noted parameters to increase the peak power coefficient from 12-15% to nearly 32% at the tip speed ratio of 0.79.

Studies by Benesh [5,6,7] have shown that improving the efficiency of Savonius wind turbine requires contributions from the lift force. Moutsoglou and Weng [8] compared the performances of both Savonius and Benesh rotors and found that the Benesh rotor has higher power and torque coefficients. The Benesh rotor is an airfoil shaped rotor, which contributes lift to the torque in the angle of attack ranging from 0-20 degrees and 180-200 degrees. Figure 1b shows the cross section of a Benesh airfoil.

The objective of the present investigation was to improve the performance of vertical axis wind turbines for producing power at a competitive rate for residential and commercial applications. Recent studies by Moutsoglou and Weng [8] suggest that increasing the efficiency of this type of turbine requires increased contribution from the lift force to generate torque. The present investigation implemented a numerical optimization technique, which have been used for optimizing highly cambered thin airfoils (which have similar shapes as high lift airfoils) for optimizing the blade shape of a vertical axis wind turbine for maximum power generation. Two optimized blade shapes were obtained and two scaled prototype models were constructed and tested in a low speed wind tunnel to compare the experimental and numerical results. The following sections include project objectives, project approach where the numerical optimization process and the experimental method are discussed, project outcomes where the results are presented and discussed, and conclusions. The public benefits to California development stage assessment, glossary and references are given following the conclusions.

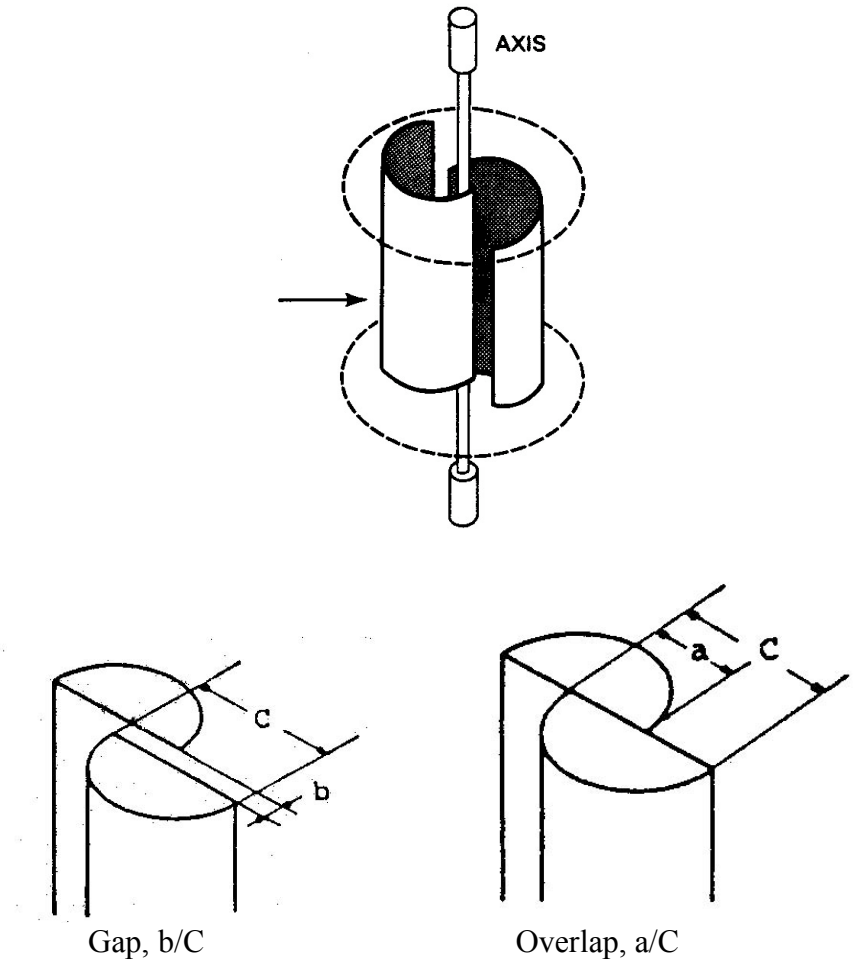

Figure 1. (a) Schematic of a Savonius vertical axis wind turbine, (b) Cross section of a Benesh airfoil.

Project Objectives

The objectives of the project were:

- Increase the efficiency of the vertical axis wind turbines by 20 – 30%.
- To lay the groundwork for development a cost effective vertical axis wind turbine that could be used for distributed power generation applications.

Numerical optimization was used to improve the geometry of a vertical axis airfoil for higher torque, which produces higher power. Two subscale models of the wind turbines with optimized airfoil were fabricated and tested in a subsonic wind tunnel to assess the numerical results and overall improvements in the power coefficient. As the results will indicate, the substantial improvements in the power coefficient make the new vertical axis wind turbine an alternative for producing power for small residential and commercial applications.

Project Approach

Project approach includes the following tasks:

Task 1. Optimization and Experiments on a Thin High Lift Mono Airfoil

Starting with an initial design (such as Benesh's profile), expressed by a set of design variables, a Computational Fluid Dynamics (CFD) code was used to compute the flow field and to optimized the torque at angles of attack varying between 0-360 deg. Then, a scale model of the optimized profile was built and tested to assess the results of the numerical investigations.

Task 2. Optimization and Experiments on a Thin High Lift Two Element Airfoil

Improvements in torque due to additional lift were further explored by using the optimized airfoil of task one with a spanwise slot at aft 25% of the airfoil. The configuration is similar to two-element airfoil, but with necessary structural rigidity required to maintain the balance of the wind turbine. Similar numerical and experimental investigations as proposed in task one of the studies were performed to assess the effects of the slot on the performance of the vertical axis wind turbine.

Aerodynamic optimization often includes three major phases. First, a baseline geometric configuration is determined and parameterized and a method of geometric manipulation is chosen. Second, the aerodynamic performance is evaluated, and then an appropriate optimization scheme is selected to obtain a desired solution. The choice in parameterization depends mostly on the nature of the geometry. A simple geometry, such as a single element airfoil might most require modification of the camber, thickness, and perhaps the maximum camber location. But a complex geometry of a Super Sonic Transport (SST), for example, may require far more parameters to sufficiently describe its geometric features.

The overall optimization method as applied to this study is illustrated in Figure 2. An initial set of values for the design variables, which in this case correspond to the baseline design, was used to define an initial configuration. For this configuration, a prescribed objective function was evaluated and the constraints were analyzed to determine whether they were violated or not. The optimizer then determined if the design was optimal, if

so, it outputs the design variables and the process terminates, and if not, the optimizer modified the design variables which were then fed back to update the design variables to generate a new configuration. This was repeated until an optimum design was obtained.

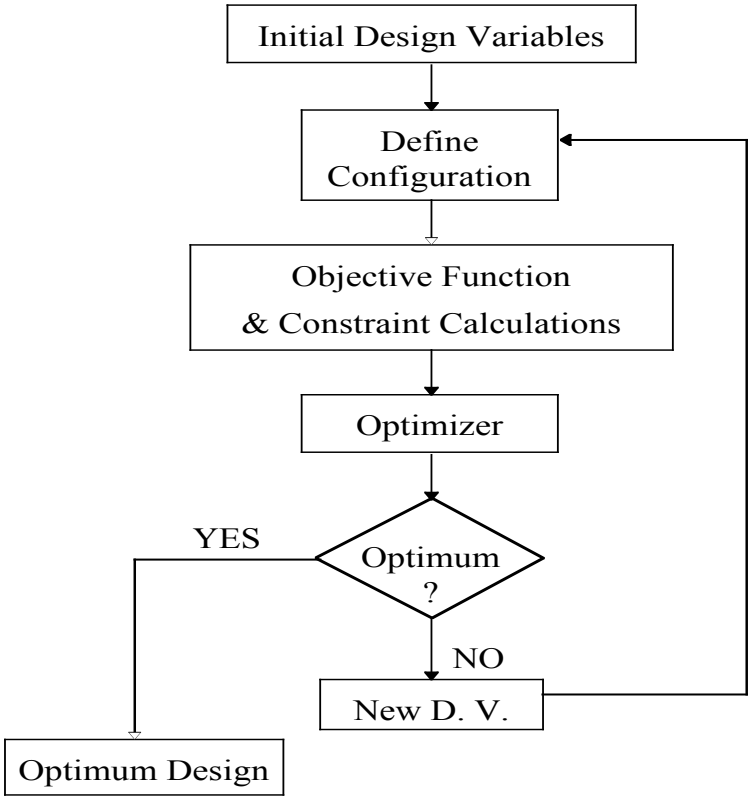

Figure 2. Optimization procedure.

The numerical optimization of a single turbine blade was initiated with a generation of a suitable high quality body fitted grid. Generation of such grid can be accomplished in several ways. For the present investigation, the grid was generated using the HEXA meshing module of the ICEMCFD software. This software allows for greater control of the grid meshing parameters, including the features that were required for the perturbation phase of the study. The baseline blade profile chosen here was the Benesh airfoil. The camber of the blade is approximated by the following equations.

$$y = \frac{m}{p^2}\left(2px - x^2\right) \qquad 0 \le x \le 0.3$$

$$y = \frac{m}{(1-p)^2}\left((1-2p) + 2px - x^2\right) \qquad 0.3 \le x \le 1.0$$

where $m = p = 0.3$

To obtain the most accurate CFD results, a small thickness was distributed along the camber line. The performance of the airfoil was not expected to change significantly with a small

thickness (2-3%). A thin profile is therefore generated by applying a constant thickness of t = 3% around camber line between $0 \le x \le 0.3$ and a tapered thickness to a closed trailing edge from $x = 0.3$. The process was described by the following equations.

For $0 \le x \le 0.3$,

$$x_u = x - 0.5t\sin\theta \qquad y_u = y + 0.5t\cos\theta$$
$$x_l = x + 0.5t\sin\theta \qquad y_l = y - 0.5t\cos\theta$$

For, $0.3 \le x \le 1.0$

$$y_t = \frac{t}{0.2}\left(ax^{\frac{1}{2}} + bx + cx^2 + dx^3 + ex^4\right)$$

a = 0.2969, b = -0.126, c = -0.3516, d = 0.2843, e = -0.1015

$$x_u = x - 0.5y_t\sin\theta \qquad y_u = y + 0.5y_t\cos\theta$$
$$x_l = x + 0.5y_t\sin\theta \qquad y_l = y - 0.5y_t\cos\theta$$

where $\theta = \tan^{-1}\left(\frac{dy}{dx}\right)$ and the subscripts u and l denote upper and lower surfaces of the blade.

To avoid computational and gird generation difficulties associated with blunt leading edges, the profile was rounded by fitting a semi-circle between the points $\left(-\frac{t}{\sqrt{5}}, \frac{t}{2\sqrt{5}}\right)$ and $\left(\frac{t}{\sqrt{5}}, -\frac{t}{2\sqrt{5}}\right)$.

The flow parameters were computed using the anticipated operational conditions of the blade for generation of about 1 KW of power. Nominal wind velocity was set at 10 m/s. The chord length of the full-scale blade was 1.8m. At standard atmospheric conditions, this translates to a Reynolds number based on the chord length of 1.233×10^6.

Not every geometric feature is modified in an optimization problem. Aerodynamic properties such as coefficients of lift and drag are usually optimized. Only geometric features that most influence the aerodynamic properties are modified to minimize computational costs. In this optimization process, a general parametric description of the baseline configuration was perturbed using a linear combination of appropriate shape functions.

We chose the Hicks-Henne shape functions [20]. They have the advantage of being space-based functions as opposed to frequency-based functions and allow for greater local control of the design. These functions have been widely used in aerodynamic optimization [9, 25].

General shape definition for this optimization is given as:

$$y(\bar{x}) = y_o(\bar{x}) + \sum_{i=1}^{S} x_i f_i(\bar{x})$$

where $\bar{x}$ is the coordinate along the airfoil blade, y_o is the y coordinate of the baseline blade, $(x_i)_{1\le i\le S}$ are the design variables, and $(f_i)_{1\le i\le S}$ are the Hicks-Henne functions.
Hicks-Henne shape functions applied in this study are given by

$$f_i = \sin\left(\pi x^{\frac{\ln(0.5)}{\ln(a)}}\right)^b$$

where a and b control the center and thickness of the perturbation, and x is the normalized coordinate along the chord. In this study, the logarithmic function, which is primarily used to alter the leading edge was not used. It was found that due to the high camber and thinness of the airfoil, small perturbations by this function propagated into excessively large displacements that affected the local shape control.

In an aerodynamic optimization process, there is a need to modify the grid around the object undergoing a geometric modification. In the work presented here, a multi-zonal grid was used and the zones that require deformations are oriented such that in any zone this was the only surface that will undergo deformation. The algebraic method is better suited for this type of grid in that the displacements applied can be interpolated within each zone thus insuring zonal compatibility. It will also allow the quality of the original grid to be preserved. It is independent from the grid generation process and can be applied to grids generated by any method. In our study, the mesh generation package ICEM/CFD was used.

Figure 3 and 4 illustrate the zoning/decomposition strategy used for the single blade and the grid used for the double optimized blades. The overlap for the two-blade configuration was 48% and the gap was zero.

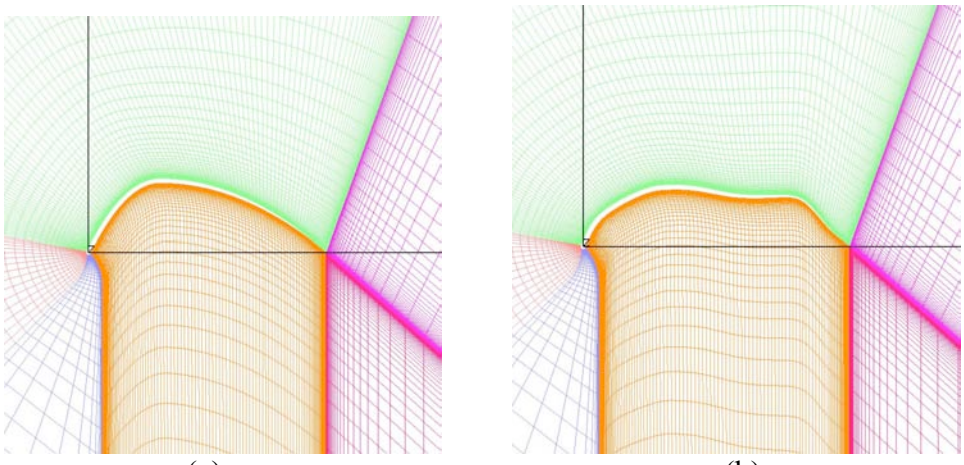

(a) (b)

Figure 3. Zones for (a) baseline blade grid, and (b) optimized blade grid.

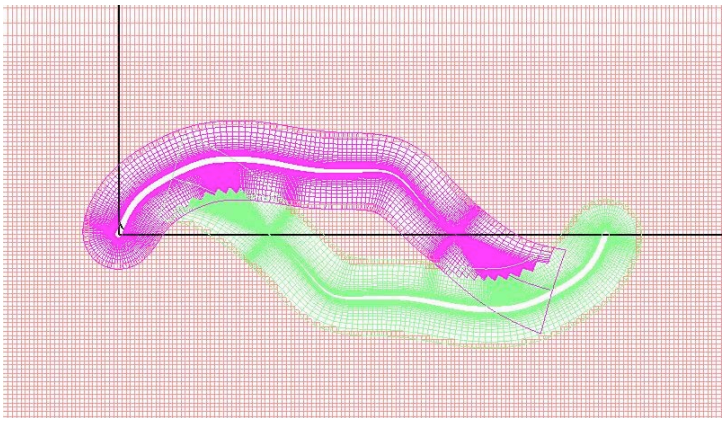

Figure 4. The optimized grid for two-blade configuration.

A non-linear Sequential Quadratic Programming scheme as implemented in I-Sight was chosen as the optimization scheme. This technique assumes that the objective function and constraints are continuously differentiable. It generates a sequence of quadratic programming sub-problems, obtained by a quadratic approximation of the Lagrangian function, and a linearization of the constraints. Second order information was updated by a quasi-Newtonian formula, and the method was stabilized by an additional line search. This type of optimization is a "sub-problem" type method and is suited for problems with many variables. The method solves a series of approximations to the following non-linear programming problem:

minimize/maximize $F(\mathbf{x})$

subject to $\mathbf{l} \le \begin{Bmatrix} \mathbf{x} \\ A\mathbf{x} \\ c(\mathbf{x}) \end{Bmatrix} \le \mathbf{u}$

where $F(\mathbf{x})$ is the objective function , is the vector that contains the design variables, contains the nonlinear constraints, and $A\mathbf{x}$ contains the linear constraint matrix. They are subjected to their corresponding lower and upper bounds contained in the vectors l and u. The method employs a nonlinear programming algorithm to search for the minimum/maximum of the objective function. Each "iteration" of the optimization consists of the following two steps. First, the solution of the nonlinear programming problem is obtained and is defined as the search direction. When this direction is determined, a line search is applied to locate a local minimum or a maximum.

In this study, the quantity to be maximized was the torque. In our analysis, the angles of attack that provide the most contribution from the lift to the torque were considered. Four angles in the vicinity of the ideal angle of attack were analyzed. The aerodynamic coefficients obtained by the flow solver were used to obtain an average torque coefficient for the angles under consideration.

This is defined as the objective function to be optimized. Constraints on the design variables were placed to ensure a smooth blade profile.

Experimental assessments of our numerical optimization were performed in the Boeing/CSULB low speed wind tunnel, which has a cross section working area of 90x120 cm and is 300 cm long. The turbine blades were built according to the optimized geometry with either a Laminate Object Machine, which is capable of fabricating objects with different contours from a CAD solid model, or shaped from brown foam with fiberglass coating. Four blades were made using the optimized geometry at 28 cm chord length and 22 cm width. Two of the blades had spanwise slots of 0.635 cm in width and 20 cm in length at 75% of the chord.
The turbine was made of two blades constrained between two round plates of either 45 or 60 cm diameter. The 45 cm diameter plates were used for an overlap ratio of 48% and the 60 cm diameter plates were used when the overlap ratio was zero.

A round shaft of approximately 1.58 cm diameter at the mid point connect the assembly to the bearing and pulley outside the wind tunnel. Figures 5 and 6 show the wind turbines with and without the slots inside the wind tunnel.

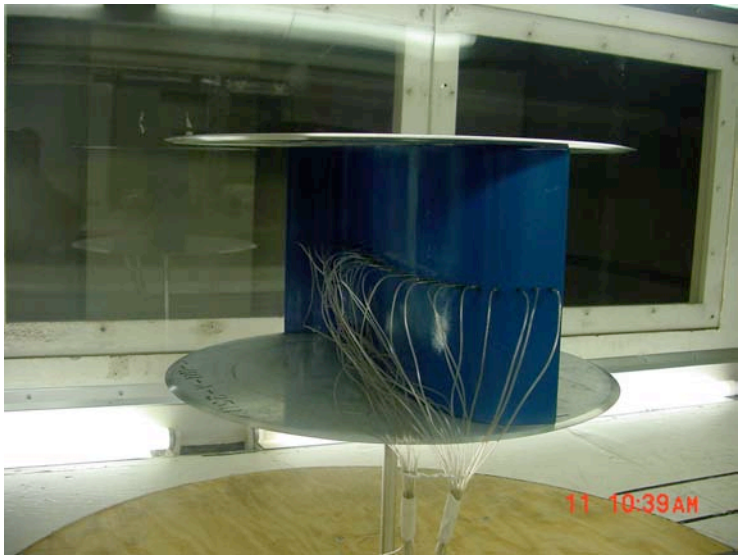

Figure 5. The wind turbine without the spanwise slots

Figure 6. The wind turbine with the spanwise slots.

Direct torque measurements were performed with a Lab-Volt electric dynamometer, which has a range of 0-27 inch-lbf. The dynamometer was connected to the shaft of the wind turbine via a belt-pulley arrangement outside the wind tunnel. Figure 7 shows the dynamometer shaft connection arrangement. The rotation speed (rpm) was measured using a Lab-Volt tachometer model EMS 8931-00 with an output range of 2 volts/1000 rpm which was attached to the shaft directly.

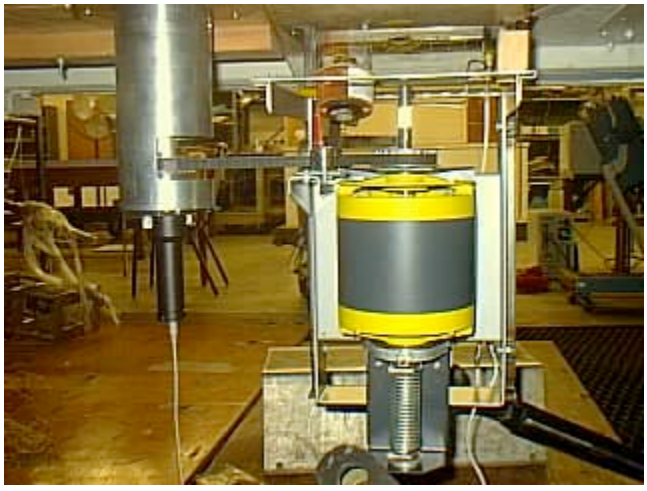

Figure 7. Dynamometer-shaft connection arrangement.

The bearing friction force or the start up force for the whole assembly was measured using a nylon chord fixed to the pulley. After winding the chord around the pulley, weights were added to the free end of the chord incrementally until it starts to rotate. The total weight amounts to the friction force. The torque was calculated by multiplying the friction force by the pulley's radius. The friction force was measured for each configuration tested.

The torque and rotation speed were measured at three free stream mean velocities of 6.8, 8, and 9.75 m/sec which correspond to Reynolds numbers based on cord length of 12.25×10^4, 14.4×10^4, 17.6×10^4 respectively. The experiments were performed for blades at zero and 48% overlap conditions. The gap between the blades was zero.

Project Outcomes

The initial values of the design variables were set at 0.0, which correspond to the unperturbed baseline blade. For each iteration of the optimization, flow field solution as well as aerodynamic coefficients were computed and analyzed. The objective function of the optimization, the torque coefficient was then computed. The aerodynamic coefficients, of lift and drag and pitching moment about the quarter chord were calculated by INS2D.

Since the blade is not used as a lifting body for an airplane configuration, but rather as a driving force of a rotating wind turbine, these forces must be resolved into appropriate normal, axial and moment components about the actual rotational axis of the turbine (Figure 8. Here A and N are axial and normal components of the forces respectively).

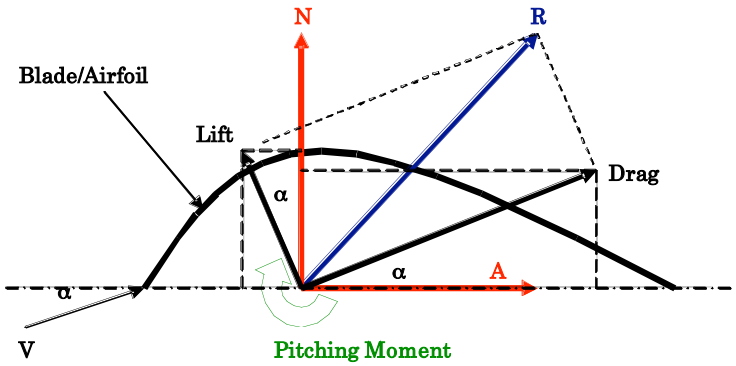

Figure 8. Resolution of aerodynamic coefficients.

Hicks-Henne functions that were used are illustrated in Figure 9. The baseline shape (in black on the bottom graph) is plotted against shapes that have been modified by the corresponding colored Hicks-Henne function (top graph). The final shape, which is ultimately used in the process, is the linear combination, which is shown by the dotted line.

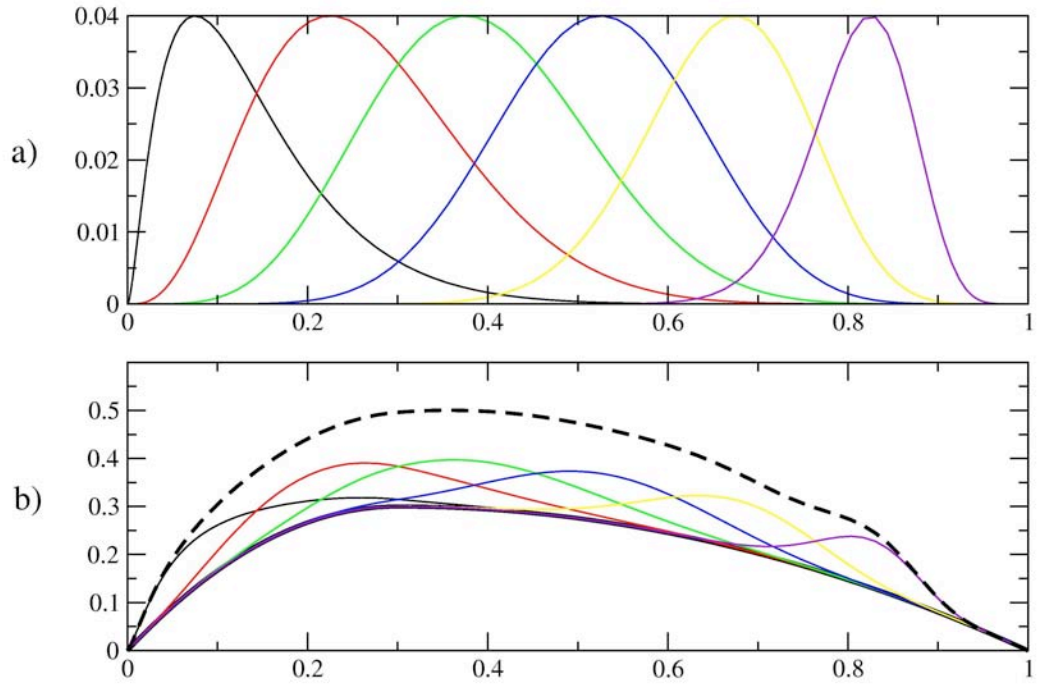

Figure 9. a) Hicks-Henne functions b) and their effects on the baseline blade.

Examination of the lift contribution for 4 angles of attack in 15-degree increments is performed to evaluate the overall effect of the optimization. The lift contribution of the blade is increased significantly in the 0-45 degrees range. For other regions where flow is almost fully separated and is thus shape-independent and the contribution from lift is negligible even for the optimized blade. When the torque coefficients at 4 different angles of attack given in Figure 10 are compared with the plot of total torque coefficient in Figure 11, they show dependence on the angle of attack. The torque coefficients also show a greater dependence when they are small and the lift curve in the region is linear as predicted by the classical aerodynamic theory.

As Figure 11 shows, the contribution of lift decreases steadily as the angle of attack increases. This trend is observed for both the optimized and the baseline blades, which is an indication of the independence of the lift contribution from the geometry at high angles of attack. This validates our initial choice of concentrating on the ideal angles of attack only.

Figure 12 shows the mean velocity contours for both the baseline and the optimized blades at 15 degrees angle of attack. For the baseline blade, the results show a very large region of flow separation and re-circulation just aft of the maximum camber location, which results in large momentum loss during its operation even at this modest angle of attack. Flow on the lower surface of the blade separates almost immediately after the leading edge creating a region of re-circulation that encompasses almost the entire lower surface. Also, there is a small separated region on the upper surface of the blade near the leading edge, but the flow quickly reattaches after that.

For the optimized blade, the area of flow separation has diminished substantially in both the upper and lower surfaces. There is no separation bubble on the upper surface and the reduced camber and the flattened top portion help to sustain an attached shear layer. Toward end flow separates briefly, but a slight arching of the blade allows reattachment. The unique arching of the blade is due to the fact that the optimization is a pure numerical phenomenon and since there are no "physical" constraints, it will find the best "numerical" result. Also, the optimization method produces a "local" optimum and cannot guarantee a global optimum. This particular shape is just one of the possibilities. The average torque coefficient, Ct, for four angles of attack for the baseline blade is 0.4167. The corresponding average coefficient for the optimized blade is 0.5211, an improvement of 23% over the baseline.

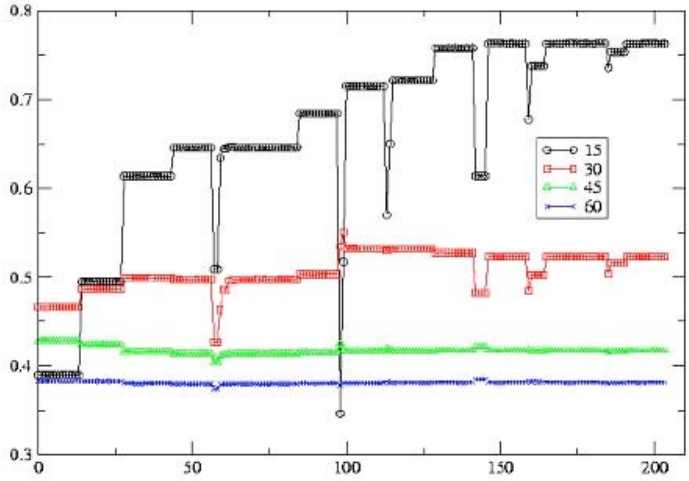

(a)

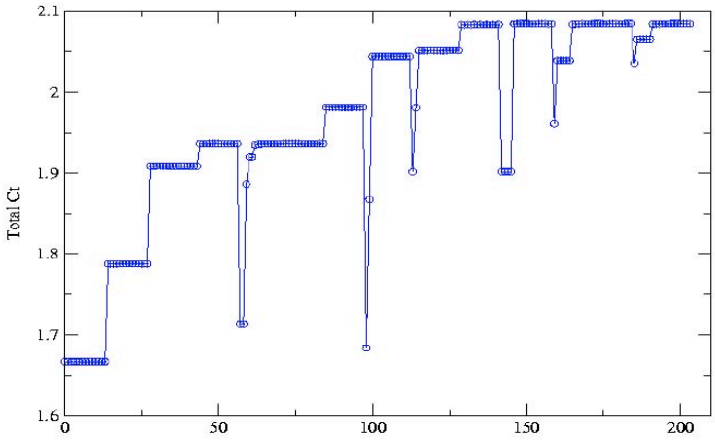

(b)

Figure 10. History of (a) torque coefficients at 15-60 angles of attack, and (b) total torque coefficient. The abscissa is the number of iterations performed before convergence.

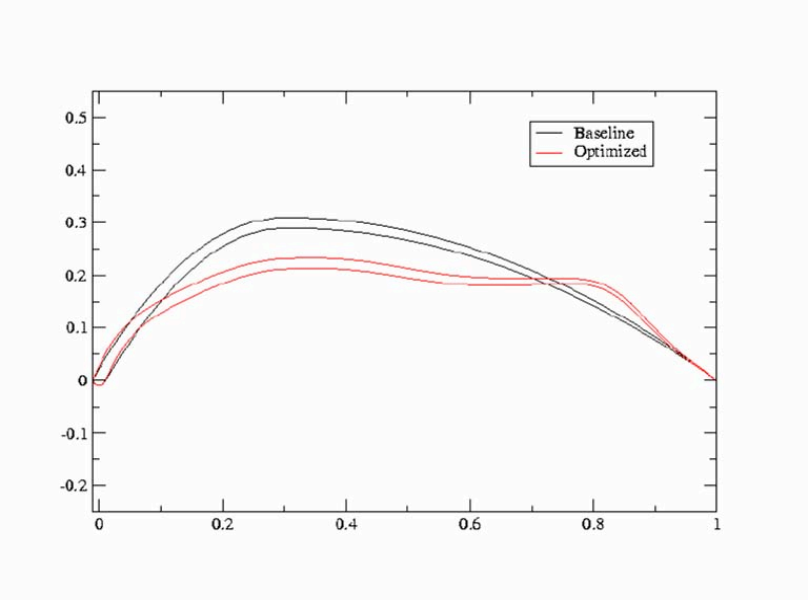

(a)

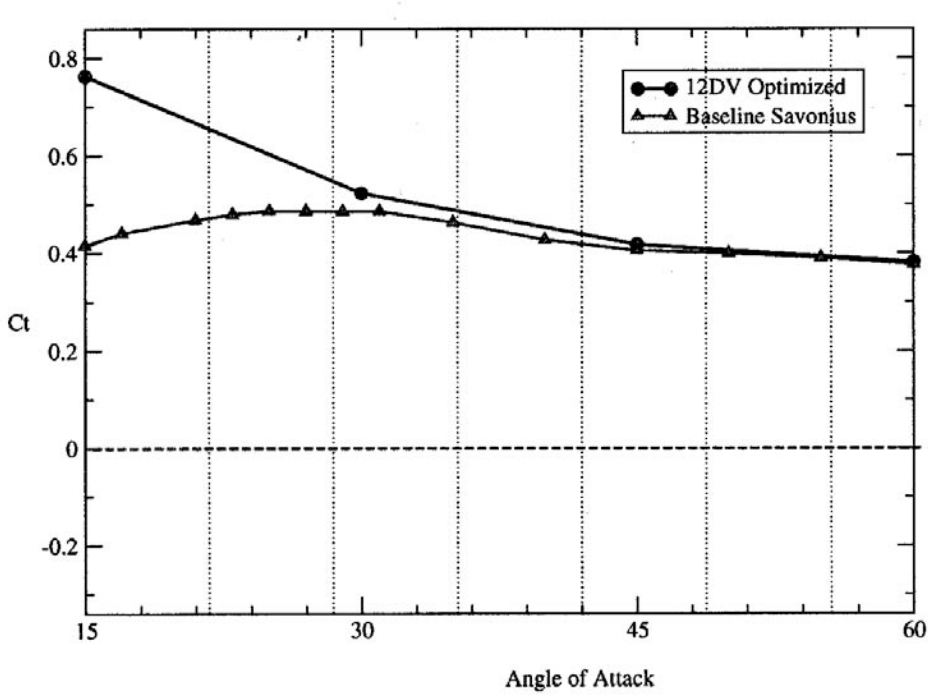

(b)

Figure 11. (a) Baseline and optimum blades profiles, and (b) Torque coefficient comparison

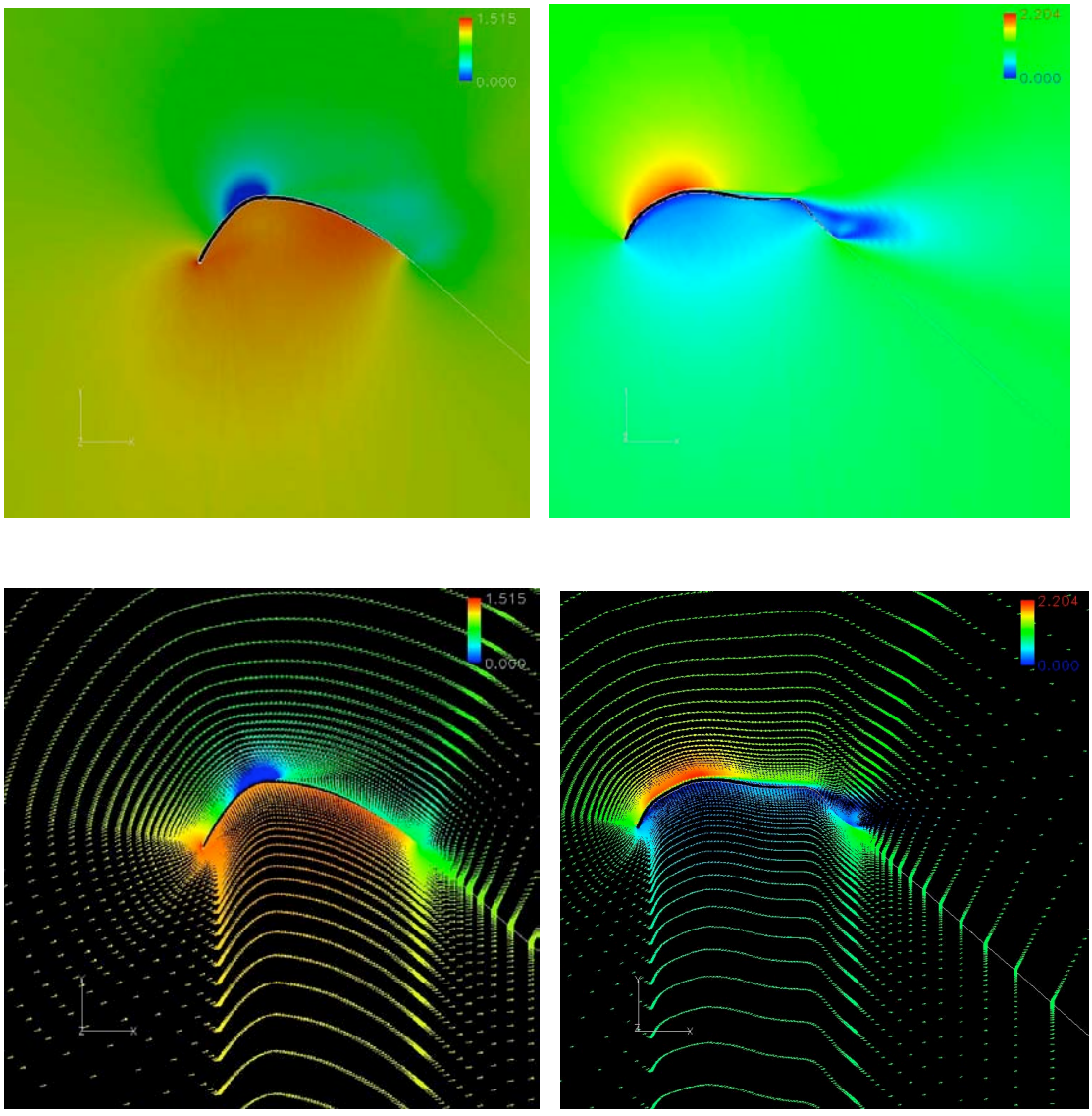

(a) (b)

Figure 12. Velocity and vector contours for (a) Baseline and (b) optimized blades at 15 degrees angles of attack.

Figure 13 shows the vector plot and the mean velocity contours for the optimized blade with the spanwise slot at 15 degrees angle of attack. For the contours, the red color means high velocity region and the dark blue area corresponds to the flow separation region. The momentum injection through the slot will increase flow separation in the in the upper side in both upstream and downstream of the slot. However, the amount of separation in the lower side is reduced significantly. The net effect of the slot is seen as loss of momentum, as compared to the corresponding case without the slot, which should results in a decrease in its overall efficiency, (lift coefficient).

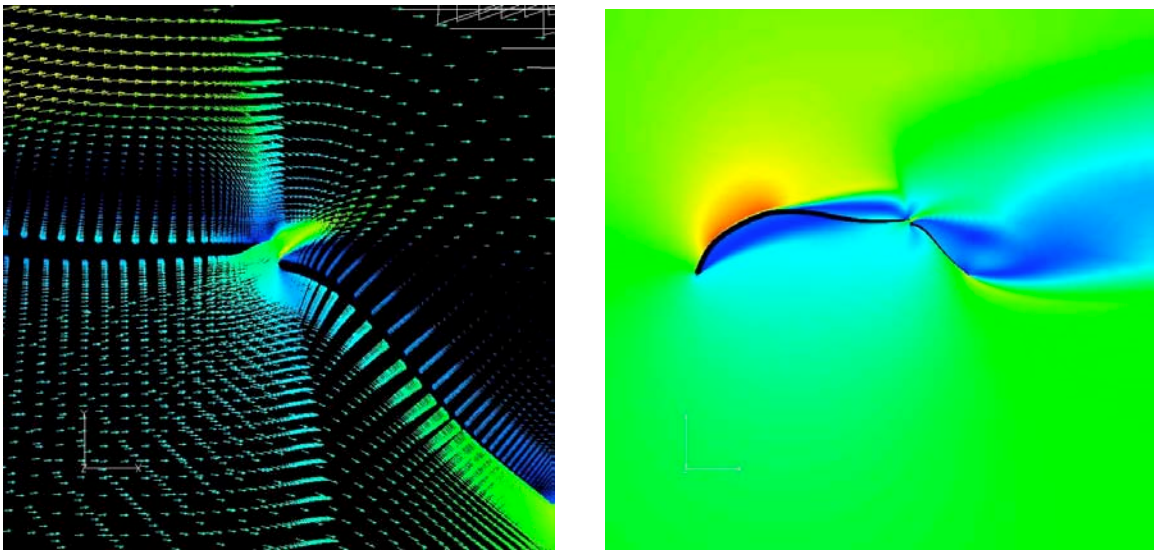

Figure 13. Vector plot and velocity contours for the optimized blade with a spanwise slot at 15 degrees angle of attack.

Figure 14 shows the mean velocity contours for the two optimized configuration at 48% overlap. Flow accelerates over and through the blades with large area of separation within the blades, near their surfaces. The separation area is higher for the lower blade than the upper one. There are also separated flow regions on the outside surfaces near the blades trailing edges. These results indicate that the high overlap region between the blades actually will induce more separation region and should not increase the overall efficiency of the two-blade configuration significantly.

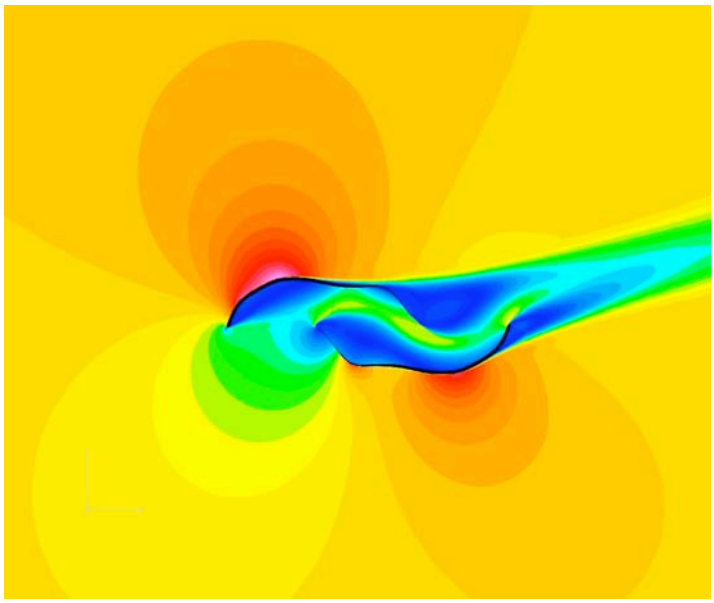

Figure 14. Velocity Contours for the two-blade system at 15 degrees angle of attack.

The results of the numerical studies indicate that the optimized single blade should produce higher torque than the baseline blade. However, the presence of the spanwise slot results in larger flow separation regions and loss of momentum which should result in reduced torque and lower performances.

For the optimized two-blade configuration with the large overlap the flow does not completely encompass the whole blades as it did for the single blade and thus should not have significant improvements in the overall drag force. For the two-blade configuration, improvement is expected when the overlap percentage is significantly reduced.

For experimental study, the focus was on the performances of the optimized two-blade configuration with and without the spanwise slots at zero and 48% overlap conditions.

Figures 15 and 16 show variation of the power coefficient for the optimized two-blade configuration with and without the spanwise slots at zero and 48% overlap conditions for the three free stream velocities of 6.8, 8.0 and 9.75 m/sec. The figures also include the corresponding results for the Savonius and Benesh airfoils tested under similar conditions taken from Moutsoglou and Weng [9]. For 48% overlap condition, the maximum power coefficients for the optimized blades are less than the corresponding values for the Savonius and Bensh airfoils. For the optimized blade, the maximum power coefficients are 0.15, 0.2, and 0.25 at about 0.8 tip speed ratio for the free stream mean velocities of 6.8, 8.0, and 9.75 m/sec. respectively. The Savonius and Benesh airfoils can sustain the maximum power coefficient for the tip speed ratio of approximately 0.8 to 1.2, while the corresponding range of the tip speed ratio for the optimized blade is at approximately 0.5 to 0.8 for the mean velocity of 6.8 m/sec and only at 0.8 for the mean velocities of 8.0 and 9.75 m/sec.

The results are changed when the overlap ratio is reduced to zero. The maximum power coefficient for the optimized blade is more than 0.4 for the mean velocities of 6.8 and 9.75 m/sec and about 0.4 for the mean velocity of 8.0 m/sec. These values are more than 30% improvements over the power coefficient of the Benesh airfoil. The rise in the power coefficients extends to a tip speed ratio of 1.6, before it starts to decrease. These results are consistent with our numerical analysis and indicate that the optimized blade can sustain power generation up to a much higher tip speed ratio than the Benesh or Savonius airfoils.

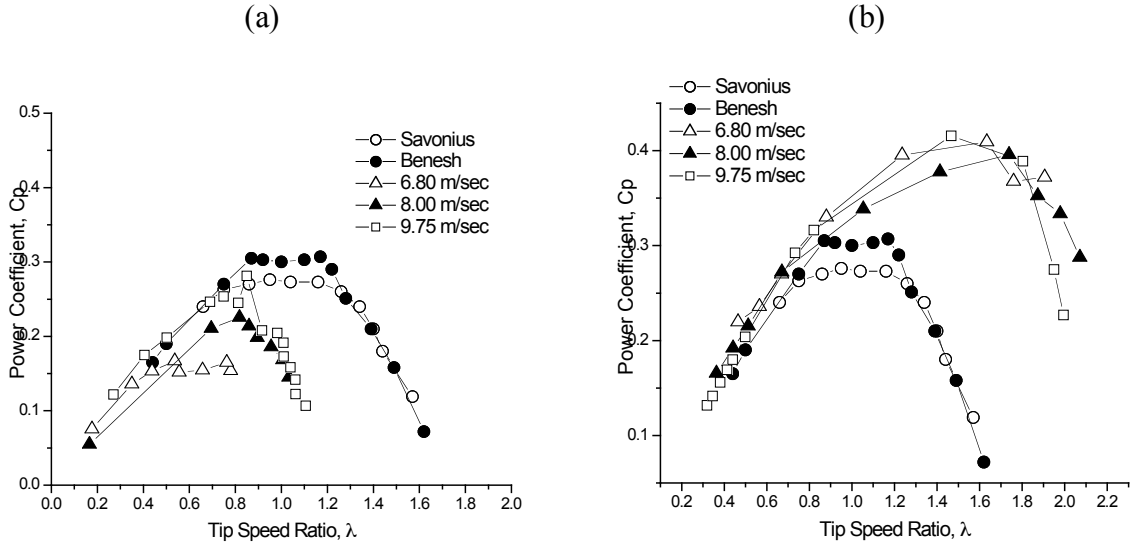

Figure 15. Variation of power coefficient at different velocities for blades without the slot at (a) 48% blade overlap and (b) zero blade overlap.

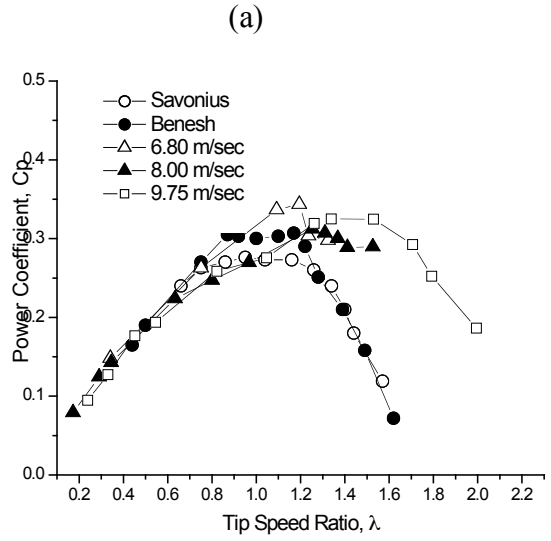

Figure 16. Variation of power coefficient at different velocities for blades with the spanwise slots at (a) 48% blade overlap and (b) zero blade overlap.

When the spanwise slots are in place, for the 48% overlap condition, the increase in the power coefficient of the optimized blades is not as significant as before. The maximum power

coefficient for the optimized blade is around 0.33 for the mean velocities of 8.0 and 9.75 m/sec, a less than 10% improvement. For the mean velocity of 6.8 m/sec, the maximum power coefficient is nearly the same as the corresponding value for the Benesh airfoil. It is interesting to note that even though the increase in the power coefficient of the optimized blades with the spanwise slots is not significant, however, the range of power production still extends to the tip speed ratio of 1.6, much higher than the corresponding value for the Benesh or Savonius airfoil.

When the overlap ratio is reduced to zero, there is more than 15% increase in the maximum power coefficient of the optimized blades as compared with the power coefficient of the Benesh airfoil at 6.8 m/sec.. However, the power coefficient is reduced by nearly 13% at velocities of 8.0 and 9.75 m/s. These results indicate that even though for the optimized blade there is an extended range of speed for the power production, however, the presence of the slots increases the regions of flow separation, and thus results in reduction of power. These results are consistent with our previous numerical analysis where more separation areas were observed on the top surface of the optimized blade with the slot in place.

Figures 17 and 18 show the corresponding torque coefficients for the results of figures 14 and 15. As the results show when the power coefficient is reduced, the torque coefficient is reduced and vise versa. These results indicate that with the optimized blades at zero overlap condition and without the spanwise slots, there are significant increases in the torque coefficient at all speeds for the tip speed ratios higher than 1.0. As before this indicates that with proper design parameters, the optimized blades can continuously generate power up to much higher tip speed ratio than the high efficiency Benesh airfoil.

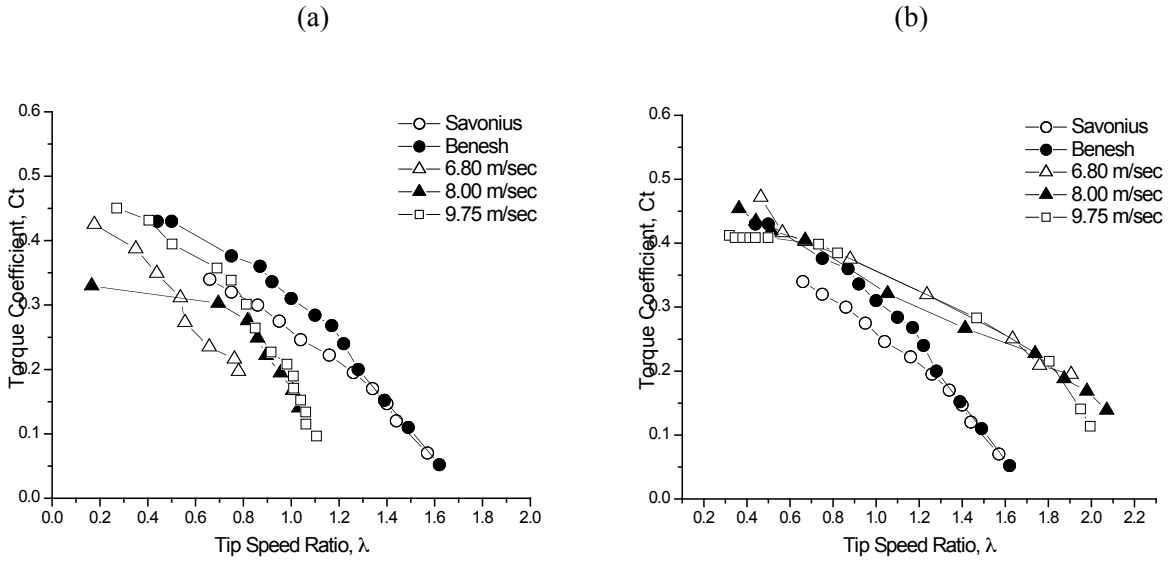

Figure 17. Variation of torque coefficient at different velocities for blades without the slot at (a) 48% blade overlap and (b) zero blade overlap.

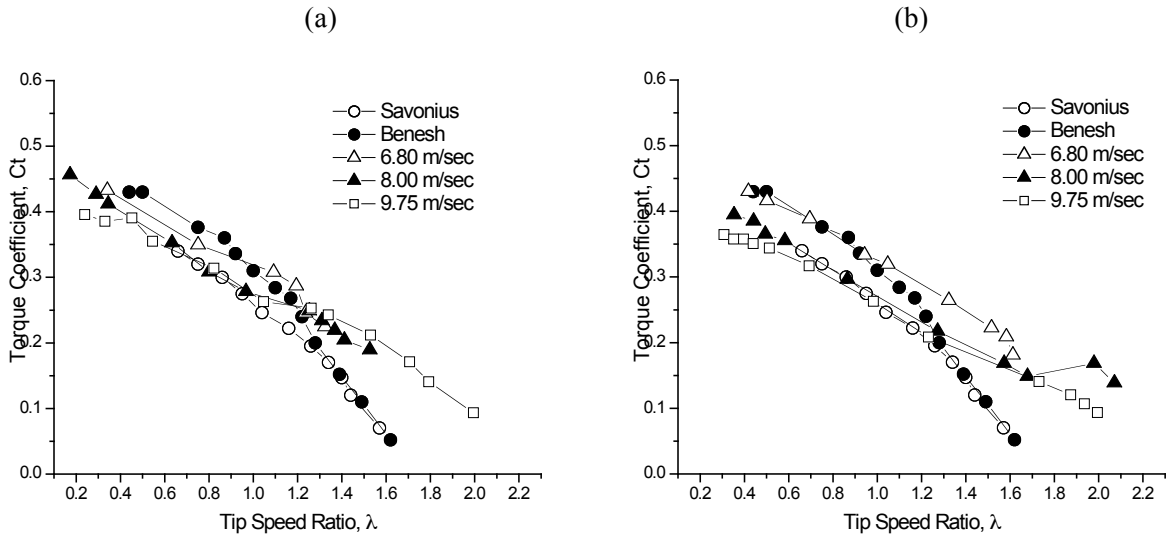

Figure 18. Variation of torque coefficient at different velocities for blades with the spanwise slots at (a) 48% blade overlap and (b) zero blade overlap.

Conclusions

A general aerodynamic optimization method was used to improve the torque characteristics of a Split-Savonius type vertical axis wind turbine. NASA INS2D software was used to compute the aerodynamic performances required to evaluate the torque characteristics. A decomposition, deformation, and reassembly method was developed to accommodate the variable geometry of the blade during the optimization process. The deformation of the grid was accomplished by a modified version of the Transfinite Interpolation (TFI) method. For the optimized blade, results of the numerical investigation showed 27% improvement in the overall torque, as compared to the corresponding value for the baseline blade.

Further numerical investigations were performed on the flow characteristics around the baseline and optimized blades, the optimized blade with spanwise slot at 75% of the chord and split type optimized blades without the slots at 48% overlap condition. Results showed reduced area of flow separation for the optimized blade. The presence of the slot resulted in increase flow separation upstream and downstream of the slot on the upper surface. However, the extent of flow separation is still less than those for the baseline blade. Results for the split-type optimized blades indicated that for increased performances, the overlap ratio should be reduced significantly.

Experimental verifications of the numerical results were made using two vertical axis small wind turbine with the optimized blades with and without the spanwise slots and at two overlap ratios of 48% and zero. The experiments were carried out in the Boeing/CSULB low speed wind tunnel

at three free stream mean velocities of 6.8, 8.0, and 9.75 m/s, which correspond to Reynolds numbers based on chord length of 12.25×10^4, 14.4×10^4, 17.6×10^4 respectively. Results show nearly 40% improvement in the maximum power coefficient for the optimized blade at zero overlap condition without the spanwise slots, as compared to the high efficiency Benesh airfoil. The increase in the power coefficient extends to a tip speed ratio of 1.6. For this configuration, there are also substantial increases in the torque coefficient for the tip speed ratios higher than 1.0, indicating that opposite to the Benesh airfoil, our wind turbine with the optimized blades can sustain high power production at higher velocities.

Recommendation

We recommend development and field-testing of two mid sized wind turbines based on the results of the present investigation. The testing should be performed near the coastal areas or/and at the top of a relatively tall building, which are in high wind shear. The testing should be performed over one year period and with daily monitoring and recording of total Kilowatt-hour along with wind speed and direction. Field-testing provides realistic information for this type of turbines before commercialization is decided upon.

Public Benefits to California

Increased focus on renewable energy has the potential for mandates by the state and national legislators for increasing its share in production of electricity. The present investigation provided significant improvement in the power coefficient of a vertical axis wind turbine. The wind turbine can be fabricated with low initial and maintenance costs to provide power at a mild wind speed of 10-15 miles per hour. The wind turbine can be scaled for different applications and levels of power generations. Installation of these wind turbines will provide substantial long-term savings to the California residence.

Development Stage Assessment

This is where you should assess where your overall development effort is in terms of the Stages and Gates process. Summarize the current development status using the Development Assessment Matrix below. Evaluate the degree to which you have completed the activities associated with each cell to include all relevant work accomplished both inside and outside of the EISG grant project. Shade in the portion of each cell that corresponds to the percent complete. The result should be a horizontal bar chart. Following the matrix, create section headings for the seven types of activities that are tracked:

- Marketing
- Engineering/Technical
- Legal / Contractual
- Risk Assessment / Quality Plans
- Strategic
- Production Readiness
- Public Benefits / Costs

Provide supporting evidence for the completion rating indicated in the matrix for each tracked activity. Provide sufficient information to allow the Program Administrator to answer the gate questions associated with each cell in which work was performed. Some of the information contained in the Conclusion and Recommendation sections will be repeated here in the appropriate sections. The EISG program is designed to primarily assist in the development of projects through Stage 3 with the highest priority being the confirmation of technical feasibility through physical testing. Projects that are successful and intend to seek follow-on funding through PIER need to show evidence of a coordinated development effort through Stage 3 to be competitive. Include relevant supporting documents (e.g., market assessment, business plan, etc.) as appendices to the final report.

Development Assessment Matrix

Stages / Activity	1 Idea Generation	2 Technical & Market Analysis	3 Research	4 Technology Develop-ment	5 Product Develop-ment	6 Demon-stration	7 Market Transfor-mation	8 Commer-cialization
Marketing								
Engineering / Technical								
Legal/ Contractual								
Risk Assess/ Quality Plans								
Strategic								
Production. Readiness/								
Public Benefits/ Cost								

1. **Marketing:** We have reviewed available market opportunities, which indicate high potentials for local electric generation in residential and commercial buildings near the coastal area, along the beaches and also between the major freeways.
2. **Engineering/Technical:** We have completed an optimization program for a high efficiency vertical axis wind turbine. The results indicate significant increase in efficiency of these types of turbines. We would like to develop two prototypes for field-testing to assess the new turbine's efficiency under real operating condition.
3. **Legal/Contractual:** We have filed a disclosure for obtaining a patent on our new wind turbine.
4. **Risk Assess/Quality Plans:** The production of the unit is fairly simple and does not pose any significant risk. The performance of the unit has been also tested in the laboratory environment. The main risk lies with the impact of actual operating environment on the unit. While some of these risk factors will be evaluated (and possibly mitigated) in the "filed test program", they may not fully represent the actual long-term environment, which these units will be working in. Rain, dirt collection and other environmental factors may reduce the performance of the unit. We expect a 10% reduction in performance without high maintenance schedule. Even with 10% reduction, we expect the high efficiency vertical axis wind turbine to provide local electric power generation at market price.
5. **Strategic:** The present innovation will reduce power grid congestion and provide opportunities to light more public areas for higher safety.
6. **Public benefits/Cost:** With the implementation of the present innovation, there will be increased energy production and reduced toxic emissions. In addition, development of these wind turbines will provide more employment opportunities, which, will be beneficial to the California's economy.
   A mid size portable high efficiency vertical axis wind turbine produces about 1KWh power in mild wind speeds of about 22 miles/hr. For coastal area on the average such wind speeds exists for more than 6 months of a year. In some other areas in California such wind speed exists throughout the year. However, assuming an average of 15 hours wind speed per day during six months period, the total power generated by a single mid size high efficiency wind turbine will be 2,700 KWh. The first time cost for a system that includes the tower and batteries installed is approximately $1095. Assuming 20 years system life and a 4% interest rate the cost per KWh produced will be about 6.5 cents. The cost is comparable in the current electric market.

References

1. Milgram, J.H., 1970, “Section Data for Thin, Highly Cambered Airfoils in Incompressible Flow,” NASA CR-1767.

2. Liebeck, R. H., and Ormsbee, A.I., 1970, ``Optimization of Airfoils for Maximum Lift, “ J. of Aircraft, Vol. 7, No. 5.

3. Liebeck, R. H., 1973, ``A Class of Airfoils Designed for High Lift in Incompressible Flow,” J. Of Aircraft, Vol. 10, No. 10.

4. Modi, V.J., and Fernando, M.S.U.K., 1989, ``On the Performance of the Savonius Wind Turbine,” J. of Solar Energy Engineering, Vol. 111, pp 71-81.

5. Benesh, A. H., 1988, ``Wind Turbine System Using a Vertical Axis Savonius Type Rotor, “ United States Patent, Patent No. 4,784,568.

6. Benesh, A. H., 1989, ``Wind Turbine System Using a Savonius Type Rotor, “ United States Patent, Patent No. 4,838,757.

7. Benesh, A. H., 1992, ``The Benesh Wind Turbine, “ SED Vol. 12, Eleventh ASME Wind Energy Symposium.

8. Moutsoglou, A., and Weng, Y., 1995, ``Performance Tests of a Benesh Wind Turbine Rotor and a Savonius Rotor,” Wind Engineering, Vol. 19, No. 6, 1995.

9. Spencer, Paul, Editor, “Small Wind Turbines,” *Refocus: International Renewable Energy Magazine*, Mar-April 2002, Elsevier Advanced Technology.

10. Gipe, Paul, *Wind Power Comes of Age*, New York, Wiley, 1995.

11. Savonius, S.J., “The S-Rotor and Its Applications,” *Mechanical Engineering*, Vol. 53, 1931, pp. 333-338.

12. Johnson, G.L., *Wind Energy Systems,* Englewood Cliffs, NJ : Prentice-Hall, c1985.

13. Blackwell, B.F., Sheldahl, R.E., and Feltz, L.V., “Wind Tunnel Performance Data for Two – and Three Bucket Savonius Rotors,” Technical Report SAND76-0131, Sandia Laboratories, Albuquerque, NM, 1977.

14. Ushiyama, Izumi and Nagai, Hiroshi, “Optimum Design Configuration and Performance of Savonius Rotors,” *Wind Engineering,* Vol.12, No.1, 1988, pp. 59-75.

15. Kahn, M. H., “Model and Prototype Performance Characteristics of Savonius Rotor Windmill,” *Wind Engineering*, Vol. 2, No.2, 1978, pp. 75-85.

16. Kim, H.-J., Sasaki, D., Obayashi, S., andNakahashi, K., “Aerodynamic Optimization of Supersonic Transport Wing Using Unstructured Adjoint Method,” *AIAA Journal*, v 39, n 6, June 2001, p 1011-1020.

17. Krist, S.L., Biedron, R.T. and Rumsey, C.L., “CFL3D User’s Manual Version 5.0,” NASA/TM-1998-208444, June 1998, NASA Langley Research Center.

18. Rogers, S.E. and Kwak, D., “Steady and Unsteady Solutions of the Incompressible Navier-Stokes Equations,” *AIAA Journal,* Vol. 29, No.4, April 1991, pp. 603-610.

19. Rogers, S.E., "A Comparison of Implicit Schemes for the Incompressible Navier-Stokes Equations with Artificial Compressibility," *AIAA Journal*, Vol. 33, No. 11, Nov. 1995, pp. 2066-2072.

20. Kim, J.E. and Klijn, N.S., "Elastic-Dynamic Rotor Blade Desgin with Mulit-Objective Optimization," *AIAA Journal*, Vol 39, No. 9, September 2001, pp. 1652-1661.

21. Cheung, S., Aaronson, P. and Edwards, T., "CFD Optimization of a Theoretical Minimum-Drag Body," *Journal of Aircraft*, Vol. 32, No. 1, January-February 1995, pp.193-198.

22. Nee, V. W., and Kovasznay, L.S.G., "The Calculation of the Incompressible Turbulent Boundary Layer by a Simple Theory," *Physics of Fluids,* Vol. 12, 1969, pp. 473-484.

23. Baldwin, B.S., and Barth, T.J., "A One-Equation Turbulence Transition Model for High Reynolds Number Wall-Bounded Flows," NASA TM-102847, 1990

24. Spalart, P.R., and Allmaras, S.R., "A One-Equation Turbulence Model for Aerodynamic Flows," *Recherche Aerospatiale,* Vol. 1, 1994, pp. 5-21.

25. Sai, V.A., and Lutfy, F.M., "Analysis of the Baldwin-Barth and Spalart-Allmaras One-Equation Turbulence Models," *AIAA Journal*, Vol. 33, No. 10, October 1995, pp. 1971-1974

26. Hicks, R. and Henne, P., "Wing Design by Numerical Optimization," *Journal of Aircraft,*Vol. 15, No. 7, July 1978, pp. 407-413.

27. Dubuc, L., Cantariti, F., Woodgate, M., Gribben, B., Badcock, K. J., and Richards, B.E., "A Grid Deformation Technique for Unsteady Flow Calculations," *Int. J. Numer. Meth. Fluids*, Vol. 32, 2000, pp. 285-311.

28. Gordon, W. J., and Hall, C.A., "Construction of Curvilinear Coordinate Systems and Applications of Mesh Generation," *Int. J. Numer. Meth. Eng.,* Vol. 7, 1973, pp. 461-477.

29. Steger, J.L., Dougherty, F.C. and J.A. Benek, "A Chimera Grid Scheme," *American Society of Mechanical Engineers, Fluids Engineering Division (Publication) FED*, Vol. 5, 1983, pp. 59-69.

30. Suhs, N.E. and Rogers, S.E., Dietz, W.E., "Pegasus5: An Automated Pre-Processor for Overset-Grid CFD," 32nd AIAA Fluid Dynamics Conference, 24-26 June, 2002, St. Louis, MO.

31. Besnard, E., Schmitz, A., Boscher, E., Garcia, N., and Cebeci, T., "Two-Dimensional Aircraft High Lift System Design and Optimization," AIAA Paper 98-404.

Glossary

A_s	Turbine Swept Area, m^2
C	Chord length, m
$C_t = \frac{T\omega}{\frac{1}{2}\rho U_\infty^3 A_s}$	Torque Coefficient
$C_p = \frac{T}{\frac{1}{2}\rho U_\infty^2 A_s R}$	Power Coefficient
R	Rotor radius of rotation
$\mathrm{Re} = \frac{U_\infty C}{\nu}$	Reynolds number
T	Torque, N-m
U_∞	Free stream mean velocity, m/s
$\lambda = \frac{R\omega}{U_\infty}$	Tip speed ratio
ρ	Air density, Kg/m^3
ν	Kinematic Viscosity,
ω	Turbine rotational speed, rpm